

Published in final edited form as:

Traffic. 2013 June ; 14(6): 650–662. doi:10.1111/tra.12064.

The Lipid Composition and Physical Properties of the Yeast Vacuole Affect the Hemifusion-Fusion Transition

Surya Karunakaran and Rutilio A. Fratti*

Department of Biochemistry, University of Illinois at Urbana-Champaign, Urbana, IL 61801

Abstract

Yeast vacuole fusion requires the formation of SNARE bundles between membranes. Although the function of vacuolar SNAREs is controlled in part by regulatory lipids, the exact role of the membrane in regulating fusion remains unclear. Because SNAREs are membrane-anchored and transmit the force required for fusion to the bilayer, we hypothesized that the lipid composition and curvature of the membrane aid in controlling fusion. Here, we examined the effect of altering membrane fluidity and curvature on the functionality of fusion-incompetent SNARE mutants that are thought to generate insufficient force to trigger the hemifusion-fusion transition. The hemifusion-fusion transition was inhibited by disrupting the 3Q:1R stoichiometry of SNARE bundles with the mutant SNARE Vam7p^{Q283R}. Similarly, replacing the transmembrane domain of the syntaxin homolog Vam3p with a lipid anchor allowed hemifusion, but not content mixing. Hemifusion-stalled reactions containing either of the SNARE mutants were stimulated to fuse with chlorpromazine, an amphipathic molecule that alters membrane fluidity and curvature. The activity of mutant SNAREs was also rescued by the overexpression of SNAREs, thus multiplying the force transferred to the membrane. Thus, we conclude that either increasing membrane fluidity, or multiplying SNARE-generated energy restored the fusogenicity of mutant SNAREs that are stalled at hemifusion. We also found that regulatory lipids differentially modulated the complex formation of wild-type SNAREs. Together, these data indicate that the physical properties and the lipid composition of the membrane affect the function of SNAREs in promoting the hemifusion-fusion transition.

Keywords

SNARE; Diacylglycerol; Lysophosphatidylcholine; Phosphoinositides; Vam7p; chlorpromazine; ergosterol; hemifusion

Introduction

The transport of cargo through the endocytic and secretory pathways is controlled by machinery that is conserved throughout eukaryotes (1). In addition, membrane fusion is essential for the release of neurotransmitters, antibodies, as well as the turnover of receptors, the destruction of pathogens and the generation of antigens (2-6). The final stage in these pathways is the fusion of membranes and transfer of cargo through a mechanism catalyzed by *N*-ethylmaleimide-sensitive factor attachment protein receptor (SNARE) proteins. All SNAREs contain a heptad-repeat termed a “SNARE motif” that is often flanked by various N-terminal domains and C-terminal membrane anchors (7). SNAREs form parallel four helical bundles through their SNARE motifs, which are primarily composed of hydrophobic

*Correspondence author: Rutilio A Fratti, Department of Biochemistry, University of Illinois at Urbana-Champaign, 419 Roger Adams Laboratory, B-4, 600 S. Mathews Ave. Urbana, IL 61801, USA, Tel.: (217) 244-5513, Fax.: (217) 244-5858, rfratti@illinois.edu.

residues with the exception of a conserved central glutamine (Q), or arginine (R) that interact in the ionic zero-layer (8). Each functional SNARE bundle is composed of 3 Q-SNARE coils and 1 R-SNARE coil. Yeast vacuole fusion depends on the Q-SNAREs Vam3p, Vam7p and Vti1p, and the R-SNARE Nyv1p. Vacuole fusion also requires the Rab GTPase Ypt7p and its effector complex HOPS (9).

Vacuole fusion occurs through a series of phases that have been experimentally defined. The fusion cascade is initiated when the AAA+ protein Sec18p (NSF) and Sec17p (α -SNAP) prime inactive cis-SNARE complexes (9, 10). Disruption of cis-SNARE complexes leads to the dissociation of Sec17p as well as the soluble SNARE Vam7p (11, 12). Between priming and fusion, membranes undergo the tethering and docking stages that are controlled by a Rab GTPase and its effector molecules, which include tethering molecules, nucleotide exchange factors, GTPase activating proteins, and Sec/Munc proteins (13). In yeast, primed vacuoles become reversibly docked through the function of Ypt7p and its effector complex HOPS (14, 15). Vacuole fusion occurs at highly organized membrane rafts termed vertex microdomains that form at the point of contact between partner vacuoles, and become enriched in the regulatory lipids and proteins required for fusion (16, 17). During the docking stage Vam7p rebinds through its interactions with the hetero-hexameric tethering complex HOPS and the lipid phosphatidylinositol 3-phosphate (PtdIns(3)P), and enters a trans-SNARE complex (18). The formation of the trans-SNARE complexes triggers the release of Ca^{2+} from the vacuole lumen (19). A penultimate step in fusion may occur through a hemifusion intermediate where the closely apposed outer membrane leaflets fuse without fusing the inner leaflets (20-22). The fusion pathway culminates with the fusion of inner leaflets and content mixing.

Vacuole fusion also requires a group of regulatory lipids that include ergosterol, diacylglycerol (DAG), phosphatidic acid (PA), as well as multiple phosphoinositides (12, 16, 23-26). Moreover, the modification of these lipids plays an important role throughout the fusion pathway. For instance, DAG is produced by the phospholipase C activity of Plc1p on PtdIns(4,5)P₂, or through the phosphatase activity of Pah1p on PA (23, 27). In both pathways the inhibition of DAG production severely inhibits vacuole fusion. The direct binding of lipids by soluble ligands can also perturb fusion at different stages of the pathway. Binding ergosterol or PtdIns(4,5)P₂ is known to inhibit at the priming stage, whereas binding PtdIns(3)P inhibits at the docking stage by preventing the re-binding of Vam7p to the membrane via its PX domain (12, 24). The role of lipids on the fusion machinery can be divided into at least two mechanisms. The first mechanism depends on the direct chemical interaction of lipids with the protein fusion catalysts, which is exemplified by the interaction of the Vam7p PX domain with PtdIns(3)P (28). The second mechanism is indirect and physical (29). This is demonstrated by the dependence of SNARE function on the assembly of metabolically active membrane raft microdomains (16). The assembly of ergosterol-rich microdomains affects the local microviscosity of the membrane and can potentially exert physical effects on the transmembrane domains (TMDs) of Vam3p, Vti1p, and Nyv1p. The concentration of specific lipids into small domains, which may increase avidity, also affects direct protein-lipid interactions and the dynamics of vacuole associated actin (16, 26).

The direct role of SNARE proteins on fusion is generally thought to occur through the transfer of energy generated from the formation of trans-SNARE complexes to the membrane and reaching the activation energy of the fusion reaction (30). Fusion is attenuated when the TMD of Vam3p or Nyv1p are exchanged for lipid anchors, or when the 3Q:1R paradigm is altered by mutating Vam7p or Nyv1p at the ionic zero layers of their SNARE motifs (31-33). The defects in triggering fusion lie downstream of trans-SNARE complex formation, leading to the hypothesis that these SNARE complexes exert

insufficient force to overcome the activation energy of fusion and may be stalled at a hemifusion stage. In this study we examined whether modifications in membrane fluidity (lateral mobility) and curvature (membrane bending), or the overexpression of SNAREs could compensate for the inability of non-fusogenic mutant SNAREs in triggering fusion. We report that non-canonical 2Q:2R SNARE complexes as well as those containing lipid-anchored Vam3p that normally do not support vacuole fusion can be stimulated to trigger fusion by altering the fluidity of the membrane to facilitate the hemifusion-fusion transition. We also found that a subset of regulatory lipids affects the assembly and function of wild type SNARE complexes and their interactions with the HOPS complex.

Results

Vam7p^{Q283R} driven fusion reactions are stalled at hemifusion

The central ionic residue of SNARE motifs is conserved throughout eukaryotes and is essential for fusion, and each fusogenic SNARE bundle is composed of 3 Q-SNAREs and 1 R-SNARE (3Q:1R). Previously, we found that point mutations yielding 2Q:2R complexes were fusion incompetent and that fusion was restored when membrane fluidity was increased with chlorpromazine (CPZ) (32). CPZ is an amphipathic small molecule that traverses the lipid bilayer and inserts itself into the inner leaflet of membranes thereby increasing the negative curvature of the outer leaflet of the bilayer in addition to increasing fluidity (34). A wealth of knowledge on the effects of CPZ on membrane physical properties has been gained from force measurements on the outer hair cell of the mammalian cochlea. CPZ decreases the steady state tethering force and increases lateral lipid mobility in outer hair cell membrane tethers (35). It also decreases the lateral cell wall tension required for vesicle generation in the plasma membrane of the outer hair cell (36). We theorize that these changes effectively lower the force required for membrane deformation and fusion to a level attainable for the 2Q:2R SNARE complex. Here, we continue to examine the regulatory role of lipid composition and curvature on SNARE function. We first compared the effects of CPZ on the ability of recombinant Vam7p to bypass anti-Sec17 antibody inhibited fusion. In these experiments, SNARE priming was inhibited with antibody against Sec17p, after which increasing concentrations of recombinant wild type Vam7p or Vam7p^{Q283R} was added to stimulate fusion. Similar to previous findings (32), we found that Vam7p^{Q283R} was unable to bypass the anti-Sec17p block (Fig. 1A, solid squares), whereas wild type Vam7p demonstrated the characteristic biphasic curve of bypass fusion with maximum activity between 50 and 100 nM (Fig. 1A, solid circles). Treating fusion reactions with CPZ prior to adding Vam7p^{Q283R} restored fusion to near wild type levels (Fig. 1A, open squares); however, this required a 10-fold increase in Vam7p^{Q283R}. Interestingly, CPZ inhibited the fusion bypass expected with low concentrations of wild type Vam7p (10-50 nM) (Fig. 1A, open circles). The inhibitory effect of CPZ on wild type Vam7p was overcome with higher concentrations of Vam7p without losing the biphasic characteristic of the curve (32, 37, 38).

Because CPZ reduced the efficacy of Vam7p at low concentrations during bypass reactions, we next tested whether CPZ altered the binding of Vam7p to the membrane. To determine this we added a dose curve of GST-Vam7p to anti-Sec17p antibody-blocked reactions in the presence or absence of CPZ. After incubation, the membrane fractions were re-isolated and probed for bound GST-Vam7p by immunoblotting. In Figure 1B we show that treatment with CPZ did not alter the binding of Vam7p to vacuoles, indicating that the differences observed in fusion were likely due to the effect of CPZ on membrane curvature and fluidity. However, these data did not indicate whether Vam7p entered into the required level of functional SNARE complexes. Vacuole extracts were also probed for the presence of membrane-anchored Ypt7p as a control for gel loading. It is possible that CPZ decreases lateral bilayer tension such that low concentrations of Vam7p, and hence low numbers of trans-SNARE pairs, were insufficient to stimulate fusion, and that this block was overcome

at higher concentrations of Vam7p. To address this, we tested whether the order in which the Vam7p and CPZ were added altered the efficacy of Vam7p in stimulating fusion. We hypothesized that the addition of Vam7p prior to CPZ would allow the soluble SNARE to form sufficient numbers of fusion competent protein complexes. Consistent with our hypothesis, we found that adding Vam7p before CPZ improved bypass fusion when compared with reactions where CPZ was added prior to Vam7p (Fig. 1C). When CPZ was added to fusion reactions that lacked anti-Sec17 antibody, we found that CPZ moderately reduced fusion whether it was added before or after exogenous GST-Vam7p (Fig. 1D). Together these data suggest that the physical properties of a membrane (e.g. fluidity and curvature changes) can modulate the efficiency of SNARE mediated fusion.

Our previous studies showed that WT and Vam7p^{Q283R} form trans-SNARE complexes successfully (32), yet fusion required a 10-fold excess of Vam7p^{Q283R} to reach WT levels of fusion (Fig. 1A). Thus, we hypothesize that Vam7p^{Q283R} forms weaker SNARE bundles that do not exert sufficient force to reach the level required for membrane deformation and hence fusion. Fusion was activated by CPZ, which has been linked with promoting the transition of membranes from a hemifused to a fully fused state and lowering the energy required for pore formation (39). Taken together, our data suggests that Vam7p^{Q283R} SNARE complexes exert insufficient force to trigger fusion following the trans-SNARE step and may be stalled in the hemifusion stage. To determine whether fusion mediated by Vam7p^{Q283R} SNARE complexes is stalled before or after the hemifusion state, and to rule out vacuole lysis as the reason for observed differences between the WT and mutant Vam7p, we used a lipid-mixing assay that measures outer leaflet fusion alone (22, 40). Here, the outer leaflets of vacuoles were labeled with Rh-PE at levels that cause self-quenching of the fluorophore. Labeled vacuoles were mixed with an excess of unlabeled vacuoles and the fusion of the outer leaflets was measured by an increase in fluorescence due to the dilution and dequenching of Rh-PE in the hemifused vacuoles. We found that following a priming block using anti-Sec17 antibody, both WT and Vam7p^{Q283R} equally supported lipid mixing in the absence of CPZ (Fig. 1E-F), suggesting that Vam7p^{Q283R} SNARE complexes are stalled at or after hemifusion. As a control, we used reactions that were inhibited with antibody against Vam3p or a mixture of Gyp1-56p and GDI to inhibit Ypt7p function. These control reactions exhibited low levels of lipid mixing, indicating that since an earlier step in fusion (priming) was inhibited, these vacuoles could not move to the lipid mixing stage (Fig. 1E). This further suggests that the effect of CPZ on content mixing occurs after the hemifusion state. In addition, these data suggest that the ionic zero-layer of SNARE complexes may serve as a checkpoint that needs to be passed to effect a transition from hemifusion to fusion. The defect in hemifusion observed with Vam7p^{Q283R} could also be a result of subtle changes in the SNARE assembly register or altered interaction with the HOPS complex. Others have shown that the rate of formation of SDS-resistant SNARE complexes where the Ionic-layer glutamine was mutated exhibited SNARE assembly kinetics similar to the WT protein suggesting that the ionic-layer residue might not be important for SNARE assembly register (41). It is however possible that the differences in SNARE assembly and disassembly kinetics in the ionic-layer mutants are subtle and need more sensitive assays. In pulldown assays, we have demonstrated that the Vam7p^{Q283R} did not affect its interaction with the HOPS complex subunits Vps11 and Vps16 (Figure 3B). Although a mutation in the ionic-layer did not affect the extent of SNARE-HOPS interaction, it is important to consider the possibility that the ionic-layer residues might be important for the stability of SNARE-HOPS interactions. It should be noted that although the final extent of lipid mixing was the same, the kinetics of our experiment seemed slower than the one reported in (42). We attributed this difference to the fact that in this experiment, lipid mixing was monitored after the addition of recombinant Vam7p following a priming block with anti-Sec17 antibody, whereas the previous report was an uninhibited reaction. It

is possible that when priming was inhibited in these reactions, there was a lag between subsequent rounds of fusion and lipid mixing and hence displays slower kinetics.

Chlorpromazine-activated fusion occurred after the lysophosphatidylcholine-sensitive fusion stage

To further determine the effects of curvature and elasticity on vacuole fusion we compared the effects of CPZ with lysophosphatidylcholine (LPC), which is an inverted cone shaped lipid and intercalates into the outer leaflet of membranes leading to an increase in both positive curvature and tension (43). Treating standard fusion reactions with LPC has been shown by others to inhibit vacuole fusion downstream of trans-SNARE complex formation (22). Here, we compared the contrasting physical effects of CPZ and LPC in the bypass of anti-Sec17 antibody blocked reactions by recombinant Vam7p. Fusion reactions were treated with buffer or anti-Sec17p antibody to block SNARE priming. Next, fusion reactions were further treated with buffer, CPZ, or LPC. As seen previously in Fig. 1, the addition of CPZ activated the fusogenic potential of Vam7p^{Q283R} (Fig. 2). In contrast to the effects of CPZ, treating with LPC blocked bypass fusion by both wild type and Vam7p^{Q283R}.

Because the order of addition altered the effects of CPZ on Vam7p-mediated bypass fusion, we tested whether pre-treating vacuoles with CPZ would nullify the inhibitory effect of LPC. When CPZ pre-treated vacuoles were subsequently treated with LPC we observed that fusion was completely inhibited to levels seen with LPC alone. Similarly, when LPC was added before CPZ treatment, bypass fusion was blocked with both wild type and mutant Vam7p (Fig. 2). Vacuole membrane fusion can itself be viewed as a two-step process: an initial fusion of the outer leaflets (cytoplasmic leaflet) and stalk formation, followed by the fusion of the inner leaflets (luminal leaflet) and fusion pore formation (39). Hemifusion could then be placed as an intermediate between these two steps, where stalk formation has occurred but inner leaflet fusion and pore formation have not. LPC has been reported to inhibit fusion by inhibiting stalk formation (44), whereas CPZ acts during the second stage of lipid mixing by promoting hemifusion-fusion transition. According to our data, the effects of LPC are dominant over the effects of CPZ because LPC inhibits the first step in lipid mixing, regardless of the order of incorporation of LPC or CPZ. The above experiment emphasizes how the shape of a lipid and hence its effect on the membrane curvature can be vital in supporting hemifusion at the sites of membrane fusion.

Increasing the number of Vam7p^{Q283R} SNARE complexes activates the hemifusion-fusion transition

The previous experiments suggested that non-canonical SNARE complexes did not exert sufficient force on the membrane and were stalled in the hemifusion stage. Thus, we hypothesized that increasing the numbers of these sub-optimal SNARE complexes (2Q:2R) on a membrane should result in sufficient force to activate the hemifusion-fusion transition. To test this hypothesis, we used yeast strains that overexpressed the four vacuole SNARE proteins to assay the efficacy of wild type and Vam7p^{Q283R} in the bypass of an anti-Sec17 antibody block. When using wild type vacuoles we found that 400 nM Vam7p rescued fusion as much as 70% of the uninhibited fusion, whereas, the Vam7p^{Q283R} mutant only partially rescued fusion (Fig. 3A; black bars). Consistent with previous figures, CPZ increased the bypass fusion by the Vam7p^{Q283R} mutant. When using vacuoles from SNARE overexpressing strains, we found that both the wild type and Vam7p^{Q283R} rescued fusion well beyond the positive control by approximately 225% and 150%, respectively (Fig. 3A; gray bars). The addition of CPZ further augmented fusion triggered by both wild type and Vam7p^{Q283R}. These data demonstrate that non-canonical SNARE complexes can generate sufficient force to trigger the hemifusion-fusion transition when the surface density of the mutant SNARE complexes is multiplied.

To determine if more SNARE complexes were formed by exogenous GST-Vam7p, SNARE complexes were affinity isolated using glutathione agarose beads. We observed a clear increase in GST-Vam7p containing complexes in the presence of excess SNAREs. However, there were no observable differences between the wild type and Vam7p^{Q283R} in the presence or absence of CPZ (Fig. 3B), indicating that the enhanced fusion was due to an increase in SNARE complex concentration. An earlier report suggests that the HOPS complex plays a more direct role in fusion by proofreading and ensuring the integrity of the trans-SNARE complexes. The authors indicate that HOPS proofreads in two stages: it inhibits the formation of mismatched 0-layer SNARE complexes and can suppress fusion with vacuoles bearing 0-layer mutations after the formation of these mismatched complexes (45). In our experiments, curiously, the increase in SNARE complexes observed with SNARE overexpression vacuoles did not correlate with an increase in the concentration of associated HOPS complex, suggesting that the excess SNARE complexes bypassed the requirement for the HOPS complex and the proofreading mechanism.

Vacuoles containing lipid-anchored Vam3p are stalled at a hemifusion intermediate

Our data thus far has indicated that the physical state (e.g. curvature and lateral tension) of the membrane affects the efficiency of the SNARE-mediated hemifusion-fusion transition. Thus, one can posit that the membrane itself could determine, though its physical properties, the force needed for SNARE-induced fusion. It is widely accepted that the formation of the helical SNARE bundle pulls and distorts the apposed membranes together to activate fusion. Here the energy generated from the formation of the SNARE complexes is transmitted to the membrane through the TMDs at the point of contact between the bilayers. Previous work by others has shown that the TMD of the vacuolar SNARE Vam3p is essential for productive priming and supporting fusion (33). In addition, cells carrying a GPI anchored hemagglutinin (HA) were stalled in the hemifusion stage and could not achieve complete fusion with red blood cells. The defect in fusion has been attributed to the absence of a TMD and the fact that the GPI anchor only traverses the outer leaflet of the bilayer (46-48). Although the sequence is not as critical, there is a stringent requirement on the length of the TMD to achieve full functionality. Truncation mutants in the TMD of HA revealed a strict requirement of at least 17 amino acids to successfully effect fusion. TMDs smaller than the critical length could not span the entire length of the bilayer and were stalled at the hemifusion stage (49).

The alpha-helical TMD of Vam3p was replaced with the isoprenylation sequence (CCIIM) of Ykt6p to make Vam3p-CCIIM (33). The lipid-anchored form of Vam3p-CCIIM is inserted into the vacuole and is present at levels similar to wild type Vam3p. Vam3p-CCIIM vacuoles accumulate cis- and trans-SNARE complexes indicating that Sec18p-dependent priming is attenuated and that trans-SNARE pairs are non-productive resulting in nearly an 80% reduction in fusion relative to wild type. We hypothesize that Vam3p-CCIIM fails to function due to a break in energy transfer between the SNARE complex and the membrane. Thus, it is likely that this mutant SNARE complex cannot transfer sufficient force to trigger the hemifusion-fusion transition. This may be due to the shortened span of the lipid anchor, which only crosses one leaflet of the bilayer. Furthermore, the defective priming seen with this mutation is likely due to the inability of Sec17p and Sec18p to correctly disrupt the cis-SNARE complex, suggesting that Vam3p-CCIIM complexes may adopt an altered conformation compared to wild type complexes.

Because membrane fusion requires the generation of sufficient energy to drive lipid rearrangement during the hemifusion-fusion transition, we hypothesized that increasing membrane fluidity would permit fusion of Vam3p-CCIIM containing vacuoles as well. To this aim, we used CPZ to lower the energy barrier and help catalyze fusion. We used vacuoles from DKY6281 and BJ3505 strains that produced Vam3p-CCIIM in standard

fusion assays. In Figure 4A we show that treatment with CPZ led to a greater than two-fold increase in fusion relative to the untreated control. Interestingly, CPZ mildly inhibited standard fusion reactions in the presence of full length Vam3p (Fig. 1D). This is also in accord with the idea that CPZ increased membrane fluidity and therefore lowered the force threshold such that the force generated by Vam3p-CCIIM would be sufficient to trigger fusion. This supports the idea that the membrane affects SNARE mediated fusion. Others have shown that the interactions of Vam3p TMDs promote the hemifusion-fusion transition (50). Thus, we posited that replacing the TMD of Vam3p with a lipid anchor would also lead to an arrest at the hemifusion-fusion state. To examine this we examined the ability of Vam3p-CCIIM to stimulate hemifusion using the aforementioned lipid-mixing assay and found that Vam3p-CCIIM vacuoles reached hemifusion similar to what was observed with WT vacuoles (Fig. 4B-C) but were defective in content mixing suggesting a defect in inner leaflet mixing. As a control, we used reactions that were inhibited with antibody against Vam3p or a mixture of Gyp1-56p and GDI to inhibit Ypt7p function. Interestingly, it has been shown that mutating the hydrophobic residues on one face of the TMD of Vam3p also results in slower inner leaflet mixing and hence hemifusion stalled liposome fusion (50). It has been demonstrated in the same study, that these residues are essential for TMD-TMD interactions that effect hemifusion-fusion transition. Another possibility is that the specific interactions between the TMD of Vam3p and certain lipids in the bilayer are abolished which could lead to a failure in membrane deformation and lipid mixing. Taken together, SNARE TMD plays a vital role in effecting hemifusion-fusion transition

Next, we performed Vam7p bypass experiments using two combinations of vacuoles. One combination contained wild type and Vam3p-CCIIM vacuoles at a 1:1 ratio, where the DKY6281 reporter strain contained wild type Vam3p and the BJ3505 reporter strain harbored Vam3p-CCIIM (Fig. 5A). The second combination used both reporter strains that harbored Vam3p-CCIIM (Fig. 5B). When we tested the effect of adding exogenous Vam7p, we found that this SNARE was unable to activate fusion using either vacuole combination. However, fusion was activated when vacuoles were treated with CPZ. Here, Vam7p^{Q283R} was also able to stimulate fusion in the presence of CPZ, albeit less efficiently than wild type Vam7p. Importantly, no combination of Vam7p and CPZ was able to stimulate fusion when both vacuole partners contained Vam3p-CCIIM (Fig. 5B).

It should be noted that the vacuoles carrying the Vam3p-CCIIM mutation accumulate cis-SNARE complexes due to a defect in priming and require the addition of exogenous Sec18p for efficient disassembly (33). An alternative explanation for Fig 5B could be construed based on the fact that in these mutants, a higher proportion of SNAREs are stuck in the cis-SNARE configuration thus resulting in fewer free SNAREs available for trans-SNARE complex formation during the Vam7p bypass reaction. If this were true, the reduced numbers of free SNAREs available for trans pairing, on either or both of the fusing partners would serve as the limiting factor for fusion and we would expect to see identical fusion profiles for Vam7p bypass reactions in the presence of CPZ with both the mixed (WT fused with Vam3p-CCIIM) and the pure Vam3p-CCIIM populations of vacuoles. We reasoned that the trans-SNARE complexes formed in 5A and 5B were equivalent in numbers and only differed in the presence or absence of at least one functional TMD. This difference was reflected in their ability to respond to CPZ treatment. Thus, we ruled out a priming defect as an explanation for the above observation and concluded that CPZ enhanced fusion with a mutant Vam3p defective in transmitting force to the bilayer.

Regulatory lipids affect the assembly of SNARE complexes and interactions with HOPS

Thus far, our data is consistent with the hypothesis that the physical properties of membranes affect fusion via the TMDs of SNAREs. In native biologically active membranes, the physical properties of the bilayer are controlled by the lipid composition

and the lateral segregation of microdomains where regulatory lipids and SNAREs interdependently assemble to promote fusion (16). These regulatory lipids are thought to modulate local curvature and fluidity at the site of fusion. In vacuoles, the fusion machinery is gathered into membrane rafts affected by a small group of chemically important lipids that include DAG, PA, ergosterol, and a panel of phosphoinositides. Here we tested whether regulatory lipids affected trans-SNARE complex formation and interactions with the HOPS tethering complex. We used well-characterized lipid-binding ligands to specifically bind and sequester lipids. PtdIns(3)P was ligated with either FYVE or PX domains. The Ent3p-ENTH domain was used to bind PtdIns(3,5)P₂ (51). PtdIns(4,5)P₂ was either bound with the Epsin 1 ENTH domain or converted to PtdIns(4)P with the bacterial PtdIns phosphatase SigD. FappPH was used to bind PtdIns(4)P. DAG was bound with C1b, and ergosterol was bound by the polyene macrolide filipin. To isolate trans-SNARE complexes, we performed fusion assays using vacuoles isolated from yeast that lacked Nyv1p and expressed Vam3p containing an internal calmodulin-binding peptide (CBP) (CBP-Vam3p *nyv1Δ*), which were incubated with DKY6281 vacuoles (*VAM3 NYV1*) (52). This ensured that the observed CBP-Vam3p-Nyv1p complexes were formed in *trans*. Following incubation CBP-Vam3p protein complexes were affinity isolated with calmodulin agarose and analyzed by immunoblotting. All of the ligands and phosphatases used resulted in potent fusion inhibition (Fig. 6A), consistent with previous reports (12, 16, 53).

Through these experiments we found that regulatory lipids had distinct roles in the formation of *trans*-SNARE complexes as well as their interactions with the HOPS complex. We found that interaction of CBP-Vam3p with Nyv1p was most sensitive to FYVE, PX, and FappPH, suggesting that PtdIns(3)P and PtdIns(4)P affect trans-SNARE pairing (Fig. 6B), in accord with findings reported by Collins and Wickner (52). We also found that C1b and filipin reduced the pairing of CBP-Vam3p and Nyv1p, demonstrating that DAG and ergosterol were also required for optimal complex formation. The PX domain blocked fusion and reduced CBP-Vam3p-Nyv1p interaction, yet had no effect on Vam7p incorporation into the remaining complex. The effect on fusion was likely due to the binding of PtdIns(3)P and HOPS complex by the Vam7p PX domain (12, 53). Surprisingly, blocking PtdIns(4)P with FappPH had a striking effect on Vam7p incorporation into SNARE complexes while the total Vam7p associated with the membrane was unaffected (not shown). This suggests that PtdIns(4)P played a role in the stabilization of the 3Q SNARE complex. Although Ent3p-ENTH potently inhibited fusion (Fig. 6A), it had no effect on trans-SNARE complex formation indicating that PtdIns(3,5)P₂ affected fusion either downstream of docking or in a parallel pathway. The exact mechanism of inhibition by Ent3p-ENTH remains uncertain. Others have found that the Ent3p-ENTH domain interacts with the N-terminal domains of Vti1p, Pep12p and Syn8p where it promotes the fusion of late endosomes (54, 55). Thus, the inhibitory nature of this domain on vacuole fusion could also be due to SNARE binding. In addition, others have shown that deleting the PI3P 5-kinase Fab1p had no effect on fusion, suggesting that generating PI(3,5)P₂ during fusion was not essential (25). However, they concluded that a regulatory influence of this lipid on the fusion machinery could not be ruled out. The role of PtdIns(4,5)P₂ was examined using the Epsin1-ENTH domain and the bacterial phosphatase SigD. We found that each reduced trans-SNARE pairing and HOPS binding to the complex. C1b and filipin both reduced Nyv1p-Vam3p interaction and blocked the incorporation of Vam7p into SNARE complexes demonstrating that DAG and ergosterol affect the formation of Vam7p-containing trans-SNARE complexes. This also suggests that Nyv1p does not require a complete 3Q-SNARE bundle to interact with Vam3p. This is keeping with a recent report showing the existence of an alternative pathway in trans-SNARE complex formation (56). Other reports have shown that blocking DAG with C1b has no effect on bulk association of Vam7p with the membrane (16), suggesting that DAG is directly required in the stabilization of the 3Q-SNARE complex and subsequent trans complex. Curiously, treating vacuoles with C1b also caused

an upward mobility shift in Vps33p; however, it is unclear whether protein modification occurred.

Vam7p bypasses the requirement for lipids that affect fusion early in the pathway

Because some regulatory lipids function in fusion before SNARE complex formation while others function downstream, we next examined whether a block on the early acting lipids could be bypassed by adding soluble Vam7p. Fusion reactions were blocked with different lipid ligands and subsequently treated with exogenously added soluble Vam7p. In Figure 7A we show that Vam7p rescued fusion reactions where PtdIns(3)P was blocked with PX, but not FYVE domain. This is likely due to the direct competition between PX and full length Vam7p. We also found that Vam7p could partially bypass blocks mediated by SigD, Epsin1-ENTH and FappPH. These data suggest that PtdIns(3)P, PtdIns(4)P, and PtdIns(4,5)P₂ function upstream of Vam7p. In contrast, Vam7p was unable to bypass blocks by C1b and filipin, suggesting that DAG and ergosterol, respectively function downstream or in parallel to Vam7p. We next examined if modulating membrane curvature and fluidity could enhance the Vam7p bypass of lipid ligand inhibition. To this end we tested whether CPZ could aid Vam7p bypass of four different lipid ligands (Fig. 7B). We found that fusion blocked by FYVE or filipin were not affected by the addition of CPZ. In contrast, CPZ enhanced the bypass of a PX block. Importantly, CPZ allowed Vam7p to bypass a C1b block. Because C1b prevents the function of DAG, which induces negative curvature and destabilizes lipid bilayers (57, 28), it is possible that the effect of CPZ could overcome the effect of DAG by promoting negative curvature and lowering the energy barrier at the site of fusion. Together these data indicate that different regulatory lipids operate upstream and downstream of Vam7p. It also illustrates that some of the lipids that act downstream of Vam7p (e.g DAG) could have an important role in maintaining the curvature of the membrane during fusion.

Discussion

In this study we examined the role of the lipid bilayer in the regulation of SNARE-mediated fusion. The effects of lipid composition and the physical properties of membranes on SNARE function have been largely overlooked. The lipid bilayer exerts two major influences on membrane-spanning proteins at a non-bonding chemical level, and non-specific interactions that occur at a physical level. In terms of physical effects, the bilayer can serve as a regulator of membrane-spanning proteins, where protein function can be affected by numerous parameters including bilayer thickness, fluidity, curvature, acyl chain packing, lateral compression, hydrophobic mismatching, and line tension (29). Membrane thickness itself can be modulated by sterol content as well as acyl chain length, and can have profound effects on protein function. Membrane raft microdomains are enriched in cholesterol/ergosterol and sphingolipids that phase separate from the bulk of the membrane (59). We hypothesize that the core fusion machinery is affected by the local physical state of the vacuolar membrane. This concept is consistent with studies showing that SNARE proteins are often found in clusters in cholesterol-rich membrane rafts as shown by microscopy, and isolation of detergent resistant rafts (60). Moreover, a growing number of studies have shown that specific lipids that influence the physical properties of membranes affect SNARE-dependent fusion, including omega-3 docosahexaenoic acid (61), sphingosine (62), cholesterol (63-65), phosphoinositides (12, 16, 25, 66, 67), DAG (23), and PA (27, 68).

SNARE-mediated fusion occurs when the formation of four alpha-helical coiled-coils release free energy. The energy is transferred through the membrane-proximal linkers and into the TMD domains, which then deform and destabilize the bilayer to surpass the force threshold required for fusion. When SNARE complexes are mutated such that the canonical 3Q:1R ratio is changed (e.g. 2Q:2R), membrane fusion is attenuated. We surmise that the

mutant SNARE complex exerts insufficient force on the membrane leading to fusion stalled at the hemifusion stage (32). We further tested this hypothesis by examining SNARE complexes where one TMD is exchanged for a lipid anchor (e.g. Vam3p-CCIIM) (31, 33). Here we showed that matching the energy barrier needed to stimulate lipid mixing with the energy released by the SNARE bundle could activate otherwise non-functional SNARE complexes. One method used in this study was the chemical treatment of membranes with the cationic amphiphile CPZ, which stimulated the hemifusion-fusion transition mediated by 2Q:2R SNARE complexes as well as those containing Vam3p-CCIIM. Because CPZ lowers membrane tension our results are in accord with the theory that lowering the force threshold of lipid mixing enables weaker SNARE bundles to stimulate the hemifusion-fusion transition. We also augmented Vam7p^{Q283R}-mediated fusion by increasing the copy number of SNARE complexes on the vacuole, suggesting that the energy generated by each mutant SNARE complex is additive in the bypass of the membrane energy barrier to stimulate fusion.

It is important to take into account recent literature that suggests hemifusion as an alternate outcome of SNARE mediated fusion rather than an on-pathway intermediate (20, 21). According to these studies, possible outcomes of a SNARE mediated fusion event could result in fast fusion-starting from point contact resulting in complete fusion, slow fusion that proceeds via stable hemifusion intermediate or a reversible kiss and run type fusion. SNARE proteins have the intrinsic capacity for full fusion, but changes in free energy resulting from membrane lipid composition or SNARE protein surface density could result in favoring one outcome more than the others (20). Taken together with results from our study, it is possible that the Vam7p^{Q283R} and Vam3p-CCIIM mutants do not generate sufficient free energy to effect complete fusion and are destined for the hemifusion pathway. The role of CPZ could then be viewed as an agent reducing the free energy threshold required for full fusion effectively tilting the balance in favor of full fusion.

Although we have shown that mutant SNAREs can be activated by chemically modulating membrane tension and curvature, it is still unclear how the assembly of the vertex microdomain controls SNARE mediated fusion. Lipid composition can change the local physical properties of the bilayer, yet the mechanisms by which these lipids affect fusion remain uncertain. Regulatory lipids such as sterols and sphingolipids serve to thicken and stiffen raft microdomains, where as others are essential for the recruitment and activation of soluble proteins (69, 70). A third function of regulatory lipids in these microdomains is the focused destabilization of the bilayer. Lipids such as DAG are known to induce negative curvature and destabilize bilayers (57, 58). The negative curvature induced by DAG and its enrichment at the vertex ring is consistent with the occurrence of a hemifusion intermediate (22). This is also in keeping with the stalk hypothesis of hemifusion where the fusion stalk contains negative curvature structures (71). Formation of the stalk is energetically disfavored by the insertion of LPC and creation of positive curvature in the outer layer of the membrane. Our finding that CPZ can overcome the inhibited fusion caused by C1b emphasizes this importance of DAG in creating negative curvature and destabilizing the membrane. We posit that binding DAG with C1b inhibits the lipid from inducing negative curvature and that CPZ restores the negative curvature needed for fusion.

The mechanism by which the membrane regulates SNAREs through a single TMD connecting to the SNARE motif via a short linker remains uncertain. However, new insights have been provided by the crystal structure of the neuronal cis-SNARE complex (72). Several new aspects of SNARE interactions were revealed, including the continuity of the alpha helices. These helices begin in the SNARE motifs and continue uninterrupted through the linkers and into the TMDs. With this knowledge, it is much easier to envision how changes in the membrane could be transferred to the SNARE motif. Furthermore, specific

interactions were found between the TMDs of syntaxin-1 and synaptobrevin-2, suggesting that interactions between the TMDs could affect the conformational arrangement of the cytoplasmic domains and regulate cis-SNARE priming. The continuity of the alpha helices coupled with the interactions of TMDs sheds some light on other studies showing that TMD of syntaxin-1 contains residues that regulate its cytoplasmic interactions with SNAP-25, a lipid anchored SNARE that lacks an alpha helical TMD (73), indicating that the syntaxin-1 TMD allosterically regulates the interaction of SNAP-25 with the cytoplasmic domain of syntaxin-1. Ungermann and colleagues showed that the TMD of the vacuolar SNARE Vam3p is essential for productive priming and supporting fusion (33). Lipid-anchored Vam3p-CCIIM vacuoles accumulate cis- and trans-SNARE complexes indicating that Sec18p-dependent priming is attenuated and that trans-SNARE pairs are non-productive resulting in a striking inhibition in fusion relative to wild type Vam3p. The lack of a TMD would inhibit the interactions of Vam3p-CCIIM with the TMDs of other vacuolar SNAREs and potentially alter the conformational structure of the cytoplasmic SNARE bundle and its productive interactions with the priming machinery. There is mounting evidence, including the results of the current study, indicating that the membrane serves as a regulator of SNARE function.

One way that membranes can modulate the allosteric effects on proteins is through changing its physical properties, which are regulated through modifications in lipid composition. This is consistent with vacuole fusion as the stoichiometry of lipid species composing the vertex microdomains are not static. Numerous lipid modifications occur through the actions of lipid kinases, phosphatases, and lipases. For example, during vacuole fusion DAG is produced by Plc1p (phospholipase C) as well as the phosphatidic acid phosphatase Pah1p (23, 27). In addition, various lipid kinases produce phosphoinositides during vacuole fusion that include PtdIns(3)P, PtdIns(4)P, PtdIns(3,5)P₂, and PtdIns(4,5)P₂ (25, 74). The dephosphorylation of phosphoinositides has also been shown to disrupt vertex microdomains and disperse SNAREs from the site of fusion (16). In addition, the genetic deletion of various phosphoinositide phosphatases yields abnormal vacuolar phenotypes, a hallmark of defective vacuole homeostasis. Among these phosphatases is the PtdIns(3)P phosphatase Ymr1p, the synaptojanin-like phosphatases Sjl2p and Sjl3p, and the PtdIns(4,5)P₂ 5-phosphatase Inp54p (75, 76). Together, these reports underscore the dependence of vacuole function and lipid modification. Although we have yet to determine the exact roles of lipid modification on vacuole SNARE function, there is growing evidence that the two are integrated in the regulation of vacuole function.

Materials and Methods

Reagents

All reagents were diluted in PS buffer (20 mM PIPES-KOH pH 6.8, 200 mM sorbitol) to a working concentration before use in any experiment. Antibodies against Nyv1p (77), Sec17p (78), Sec18p (11), Vam3p (79) have been described previously. Chlorpromazine (Sigma) was stored as a 4.5 mM stock solution in DMSO. Lysophosphatidyl choline (Sigma) was stored at a stock concentration of 1% (wt/vol) in 100% ethanol. Filipin was dissolved in DMSO at a stock concentration of 10 mM and used at a final concentration of 20 μ M.

Recombinant proteins

Recombinant GST-Vam7p (wild type and Q283R) was purified and dialyzed into PS buffer with 125 mM KCl as described (32, 37). The lipid binding domains GST-C1b (80), GST-FYVE (81), GST-PX (12), GST-Ent3p-ENTH (a gift from S. Friant, Institut de biologie et chimie des proteines, Lyon, FR) (51), GST-Epsin1-ENTH (82), MBP-FappPH (53), His₆-

MTM-1 (83), His₆-SigD (84), His₆-Gyp1-56 (85), GDI (86) were purified as previously described.

Strains

BJ3505 (*MATa pep4::HIS3 prb1-Δ1.6R his3-200 lys2-801 trp1Δ101(gal3) ura3-52 gal2 can1*) and DKY6281 (*MATa leu2-3 leu2-112 ura3-52 his3-Δ200 trpΔ1-901 lys 2-801*) were used for standard vacuole fusion assays (87). The Vam3p-CCIIIM strains carry a chimeric Vam3p where the transmembrane domain was replaced with the farnesylation site from Ykt6p (33). Yeast strains overexpressing the four vacuolar SNAREs under the control of an ADH promoter (A gift from V. Starai, University of Georgia) were used in Vam7p bypass fusion reactions (86). BJ3505 CBP-Vam3p *nyv1Δ* was used for isolating trans-SNARE complexes (52).

Vacuole Isolation and in vitro vacuole fusion

Vacuoles were isolated from yeast strains by floatation (88). Fusion reactions (30 μl) contained 3 μg each of vacuoles from BJ3505 (*pep4Δ PHO8*) and DK6281 (*PEP4 pho8Δ*), fusion assay buffer (125 mM KCl, 5 mM MgCl₂, 20 mM PIPES-KOH pH 6.8, 200 mM sorbitol), ATP regenerating system (1 mM ATP, 29 mM creatine phosphate, 0.1 mg/ml creatine kinase), 10 μM CoA and 283 nM IB2. Reactions were incubated at 27°C for 90 minutes and the Pho8p activity was measured in 250 mM Tris-Cl PH 8.5, 0.4% Triton X-100, 10 mM MgCl₂, 1 mM *p*-nitrophenylphosphate. During fusion, the Pep4p protease gains access to the pro-alkaline phosphatase (proPho8p) and cleaves it to form mature alkaline phosphatase. The quantity of *p*-nitrophenylate produced was measured at 400 nm. One unit of fusion was defined as 1 μmol of *p*-nitrophenylate produced minute⁻¹ μg⁻¹ of *pep4Δ* vacuoles.

Vam7p bypass fusion reaction

Fusion reactions were incubated at 27°C with 85 μg/ml α-Sec17 antibody to block priming. After 15 minutes, 150 μM chlorpromazine (CPZ) or 0.033% lysophosphatidylcholine (LPC) was added and the reactions were incubated for 5 minutes before the addition of Vam7p or Vam7p^{Q283R}. The reactions were incubated for an additional 70 minutes and assayed for alkaline phosphatase activity.

Trans-SNARE complex Isolation

Trans-SNARE complexes were isolated and analyzed as described with some minor modifications (38, 52). Large-scale 16X (480 μl) fusion reactions containing 48 μg of vacuoles from BJ3505 CBP-Vam3p *nyv1Δ* and 48 μg of vacuoles from DK6281 backgrounds were incubated in the presence of buffer or different lipid binding domains (10 μM Ent3p-ENTH, 10 μM GST-Epsin1-ENTH, 25 μM GST-PX, 2 μM His₆-SigD, 1 μM MBP-FappPH, 20 μM Filipin, 10 μM GST-C1b or 2 μM GST-FYVE). After incubation at 27°C for 90 minutes, reactions were placed on ice for 5 minutes and 30 μl was withdrawn from each sample to assay Pho8p activity. The remaining samples were centrifuged (16,000 g, 15 minutes, 4°C) to sediment the vacuoles and the supernatants were discarded. Vacuole pellets were overlaid with 200 μl ice-cold solubilization buffer (20 mM Tris-Cl pH 7.5, 150 mM NaCl, 1 mM MgCl₂, 0.5% Triton X-100 and 20% glycerol) with protease inhibitors (0.46 μg/ml leupeptin, 3.5 μg/ml pepstatin, 2.4 μg/ml Pefabloc-SC and 1 mM PMSF) and gently resuspended. Solubilization buffer was added to a final volume of 400 μl and the extracts were mixed by nutating at 4°C. After 20 minutes, insoluble debris was removed by centrifugation (16,000 g, 20 minutes, 4°C). Supernatants were transferred to fresh tubes and 10% of the extract was saved for input samples. The remaining extracts were brought up to 2 mM CaCl₂ and incubated with 40 μl calmodulin Sepharose beads equilibrated with

solubilization buffer (GE Healthcare; 4°C, 12 h, nutating). The beads were collected by centrifugation (3,000 g, 2 minutes, 4°C) and washed five times with 1 ml of solubilization buffer containing 1% Triton and 2 mM CaCl₂ followed by bead centrifugation. Bound proteins were eluted with solubilization buffer containing 0.1% Triton X-100 and 5 mM EGTA. The eluents were mixed with SDS sample buffer and used for SDS-PAGE analysis and immunoblotting.

Lipid mixing

Lipid mixing assays were conducted using Rhodamine conjugated phosphatidylethanolamine (Rh-PE; Invitrogen) as described with minor modification (27). BJ3505 background vacuoles (300 µg) were incubated in 400 µl of PS buffer containing 150 µM Rh-PE (10 minutes, 4°C, nutating). Samples were mixed with 15% Ficoll in PS buffer (wt/vol) and transferred to an ultracentrifuge tube (11 × 60 mm). Samples were overlaid with 1.0 ml each of 8%, 4%, and 0% Ficoll. Labeled vacuoles were re-isolated by centrifugation (105,200 g, 25 minutes, 4°C) and recovered from the 0 - 4%-Ficoll interface. Lipid mixing assays (90 µl) contained 2 µg of Rh-PE-labeled vacuoles and 16 µg of unlabeled vacuoles in fusion buffer. Reaction mixtures were transferred to a black, half-volume 96-well flat-bottom microtiter plate on ice. Reactions were started by transferring the plate to a fluorescence plate reader set at 27°C. Measurements were taken every minute for 60 minutes, yielding fluorescence values at the onset (F_0) and during the reaction (F_t). The final 10 measurements of a sample after adding 0.33% (vol/vol) Triton X-100 were averaged and used as a value for the fluorescence after infinite dilution (F_{TX100}). The relative total fluorescence change $\Delta F_t / F_{TX100} = (F_t - F_0) / F_{TX100}$ was calculated.

Acknowledgments

We thank Drs. William Wickner and Alexey Merz for generous gifts of antisera and Drs. Vincent Starai, Sylvie Friant, and Alexey Merz for strains and plasmids. We also thank Dr. Vincent Starai, Dr. Joanna Shisler, Dr. Nancy Beck, and members of the Fratti Lab for critical reading of the manuscript. This research was supported by a Basil O'Connor Starter Scholar Research Award from the March of Dimes Birth Defects Foundation to RAF (5-FY09-117), a grant from the University of Illinois Research Board awarded to RAF, and a grant from the National Institutes of Health (GM101132) to RAF.

References

1. Jahn R, Sudhof TC. Membrane fusion and exocytosis. *Annu Rev Biochem.* 1999; 68:863–911. [PubMed: 10872468]
2. Bonifacino JS, Glick BS. The mechanisms of vesicle budding and fusion. *Cell.* 2004; 116(2):153–166. [PubMed: 14744428]
3. Wickner W, Schekman R. Membrane fusion. *Nat Struct Mol Biol.* 2008; 15(7):658–664. [PubMed: 18618939]
4. Alix E, Mukherjee S, Roy CR. Subversion of membrane transport pathways by vacuolar pathogens. *J Cell Biol.* 2011; 195(6):943–952. [PubMed: 22123831]
5. Schorey JS, Bhatnagar S. Exosome function: from tumor immunology to pathogen biology. *Traffic.* 2008; 9(6):871–881. [PubMed: 18331451]
6. Chirivino D, Del Maestro L, Formstecher E, Hupe P, Raposo G, Louvard D, Arpin M. The ERM proteins interact with the HOPS complex to regulate the maturation of endosomes. *Mol Biol Cell.* 2011; 22(3):375–385. [PubMed: 21148287]
7. Jahn R, Scheller RH. SNAREs - engines for membrane fusion. *Nat Rev Mol Cell Biol.* 2006
8. Fasshauer D, Sutton RB, Brunger AT, Jahn R. Conserved structural features of the synaptic fusion complex: SNARE proteins reclassified as Q- and R-SNAREs. *Proc Natl Acad Sci U S A.* 1998; 95(26):15781–15786. [PubMed: 9861047]

9. Wickner W. Membrane Fusion: Five Lipids, Four SNAREs, Three Chaperones, Two Nucleotides, and a Rab, All Dancing in a Ring on Yeast Vacuoles. *Annu Rev Cell Dev Biol.* 2010; 26:115–136. [PubMed: 20521906]
10. Sollner T, Bennett MK, Whiteheart SW, Scheller RH, Rothman JE. A protein assembly-disassembly pathway in vitro that may correspond to sequential steps of synaptic vesicle docking, activation, and fusion. *Cell.* 1993; 75(3):409–418. [PubMed: 8221884]
11. Mayer A, Wickner W, Haas A. Sec18p (NSF)-driven release of Sec17p (alpha-SNAP) can precede docking and fusion of yeast vacuoles. *Cell.* 1996; 85(1):83–94. [PubMed: 8620540]
12. Boeddinghaus C, Merz AJ, Laage R, Ungermann C. A cycle of Vam7p release from and PtdIns 3-P-dependent rebinding to the yeast vacuole is required for homotypic vacuole fusion. *J Cell Biol.* 2002; 157(1):79–89. [PubMed: 11916982]
13. Zerial M, McBride H. Rab proteins as membrane organizers. *Nat Rev Mol Cell Biol.* 2001; 2(2):107–117. [PubMed: 11252952]
14. Seals DF, Eitzen G, Margolis N, Wickner WT, Price A. A Ypt/Rab effector complex containing the Sec1 homolog Vps33p is required for homotypic vacuole fusion. *Proc Natl Acad Sci U S A.* 2000; 97(17):9402–9407. [PubMed: 10944212]
15. Mayer A, Wickner W. Docking of yeast vacuoles is catalyzed by the Ras-like GTPase Ypt7p after symmetric priming by Sec18p (NSF). *J Cell Biol.* 1997; 136(2):307–317. [PubMed: 9015302]
16. Fratti RA, Jun Y, Merz AJ, Margolis N, Wickner W. Interdependent assembly of specific regulatory lipids and membrane fusion proteins into the vertex ring domain of docked vacuoles. *J Cell Biol.* 2004; 167(6):1087–1098. [PubMed: 15611334]
17. Wang L, Seeley ES, Wickner W, Merz AJ. Vacuole Fusion at a Ring of Vertex Docking Sites Leaves Membrane Fragments within the Organelle. *Cell.* 2002; 108(3):357–369. [PubMed: 11853670]
18. Ungermann C, Sato K, Wickner W. Defining the functions of trans-SNARE pairs. *Nature.* 1998; 396(6711):543–548. [PubMed: 9859990]
19. Merz AJ, Wickner W. *Trans*-SNARE interactions elicit Ca²⁺ efflux from the yeast vacuole lumen. *J Cell Biol.* 2004; 164:195–206. [PubMed: 14734531]
20. Giraudo CG, Hu C, You D, Slovic AM, Mosharov EV, Sulzer D, Melia TJ, Rothman JE. SNAREs can promote complete fusion and hemifusion as alternative outcomes. *J Cell Biol.* 2005; 170(2):249–260. [PubMed: 16027221]
21. Diao J, Grob P, Cipriano DJ, Kyoung M, Zhang Y, Shah S, Nguyen A, Padolina M, Srivastava A, Vrljic M, Shah A, Nogales E, Chu S, Brunger AT. Synaptic proteins promote calcium-triggered fast transition from point contact to full fusion. *elife.* 2012; 1:e00109. [PubMed: 23240085]
22. Reese C, Mayer A. Transition from hemifusion to pore opening is rate limiting for vacuole membrane fusion. *J Cell Biol.* 2005; 171(6):981–990. [PubMed: 16365164]
23. Jun Y, Fratti RA, Wickner W. Diacylglycerol and its formation by Phospholipase C regulate Rab- and SNARE- dependent yeast vacuole fusion. *J Biol Chem.* 2004; 279:53186–53195. [PubMed: 15485855]
24. Kato M, Wickner W. Ergosterol is required for the Sec18/ATP-dependent priming step of homotypic vacuole fusion. *Embo J.* 2001; 20(15):4035–4040. [PubMed: 11483507]
25. Mayer A, Scheglmann D, Dove S, Glatz A, Wickner W, Haas A. Phosphatidylinositol 4,5-bisphosphate regulates two steps of homotypic vacuole fusion. *Mol Biol Cell.* 2000; 11(3):807–817. [PubMed: 10712501]
26. Karunakaran S, Sasser T, Rajalekshmi S, Fratti RA. SNAREs, HOPS, and regulatory lipids control the dynamics of vacuolar actin during homotypic fusion. *J Cell Sci.* 2012
27. Sasser T, Qiu QS, Karunakaran S, Padolina M, Reyes A, Flood B, Smith S, Gonzales C, Fratti RA. Yeast lipin 1 orthologue pah1p regulates vacuole homeostasis and membrane fusion. *J Biol Chem.* 2012; 287(3):2221–2236. [PubMed: 22121197]
28. Cheever ML, Sato TK, de Beer T, Kutateladze TG, Emr SD, Overduin M. Phox domain interaction with PtdIns(3)P targets the Vam7 t-SNARE to vacuole membranes. *Nat Cell Biol.* 2001; 3(7):613–618. [PubMed: 11433291]
29. Andersen OS, Koeppe RE 2nd. Bilayer thickness and membrane protein function: an energetic perspective. *Annu Rev Biophys Biomol Struct.* 2007; 36:107–130. [PubMed: 17263662]

30. Chernomordik LV, Kozlov MM. Mechanics of membrane fusion. *Nat Struct Mol Biol.* 2008; 15(7):675–683. [PubMed: 18596814]
31. Jun Y, Xu H, Thorngren N, Wickner W. Sec18p and Vam7p remodel trans-SNARE complexes to permit a lipid-anchored R-SNARE to support yeast vacuole fusion. *Embo J.* 2007; 26(24):4935–4945. [PubMed: 18007597]
32. Fratti RA, Collins KM, Hickey CM, Wickner W. Stringent 3Q: 1R composition of the SNARE 0-layer can be bypassed for fusion by compensatory SNARE mutation or by lipid bilayer modification. *J Biol Chem.* 2007; 282(20):14861–14867. [PubMed: 17400548]
33. Rohde J, Dietrich L, Langosch D, Ungermann C. The transmembrane domain of Vam3 affects the composition of cis- and trans-SNARE complexes to promote homotypic vacuole fusion. *J Biol Chem.* 2003; 278(3):1656–1662. [PubMed: 12427733]
34. Fang J, Iwasa KH. Effects of chlorpromazine and trinitrophenol on the membrane motor of outer hair cells. *Biophys J.* 2007; 93(5):1809–1817. [PubMed: 17483184]
35. Murdock DR, Ermilov SA, Spector AA, Popel AS, Brownell WE, Anvari B. Effects of chlorpromazine on mechanical properties of the outer hair cell plasma membrane. *Biophys J.* 2005; 89(6):4090–4095. [PubMed: 16199506]
36. Morimoto N, Raphael RM, Nygren A, Brownell WE. Excess plasma membrane and effects of ionic amphipaths on mechanics of outer hair cell lateral wall. *Am J Physiol Cell Physiol.* 2002; 282(5):C1076–86. [PubMed: 11940523]
37. Fratti RA, Wickner W. Distinct Targeting and Fusion Functions of the PX and SNARE Domains of Yeast Vacuolar Vam7p. *J Biol Chem.* 2007; 282(17):13133–13138. [PubMed: 17347148]
38. Qiu QS, Fratti RA. The Na⁺/H⁺ exchanger Nhx1p regulates the initiation of *Saccharomyces cerevisiae* vacuole fusion. *J Cell Sci.* 2010; 123(Pt 19):3266–3275. [PubMed: 20826459]
39. Melikyan GB, Brener SA, Ok DC, Cohen FS. Inner but not outer membrane leaflets control the transition from glycosylphosphatidylinositol-anchored influenza hemagglutinin-induced hemifusion to full fusion. *J Cell Biol.* 1997; 136(5):995–1005. [PubMed: 9060465]
40. Reese C, Heise F, Mayer A. Trans-SNARE pairing can precede a hemifusion intermediate in intracellular membrane fusion. *Nature.* 2005; 436(7049):410–414. [PubMed: 15924133]
41. Scales SJ, Yoo BY, Scheller RH. The ionic layer is required for efficient dissociation of the SNARE complex by alpha-SNAP and NSF. *Proc Natl Acad Sci U S A.* 2001; 98(25):14262–14267. [PubMed: 11762430]
42. Jun Y, Wickner W. Assays of vacuole fusion resolve the stages of docking, lipid mixing, and content mixing. *Proc Natl Acad Sci U S A.* 2007; 104(32):13010–13015. [PubMed: 17664431]
43. Yoo J, Cui Q. Curvature generation and pressure profile modulation in membrane by lysolipids: insights from coarse-grained simulations. *Biophys J.* 2009; 97(8):2267–2276. [PubMed: 19843459]
44. Gunther-Ausborn S, Praetor A, Stegmann T. Inhibition of influenza-induced membrane fusion by lysophosphatidylcholine. *J Biol Chem.* 1995; 270(49):29279–29285. [PubMed: 7493959]
45. Starai VJ, Hickey CM, Wickner W. HOPS proofreads the trans-SNARE complex for yeast vacuole fusion. *Mol Biol Cell.* 2008; 19(6):2500–2508. [PubMed: 18385512]
46. Kemble GW, Danieli T, White JM. Lipid-anchored influenza hemagglutinin promotes hemifusion, not complete fusion. *Cell.* 1994; 76(2):383–391. [PubMed: 8293471]
47. Melikyan GB, White JM, Cohen FS. GPI-anchored influenza hemagglutinin induces hemifusion to both red blood cell and planar bilayer membranes. *J Cell Biol.* 1995; 131(3):679–691. [PubMed: 7593189]
48. Kemble GW, Henis YI, White JM. GPI- and transmembrane-anchored influenza hemagglutinin differ in structure and receptor binding activity. *J Cell Biol.* 1993; 122(6):1253–1265. [PubMed: 8397215]
49. Armstrong RT, Kushnir AS, White JM. The transmembrane domain of influenza hemagglutinin exhibits a stringent length requirement to support the hemifusion to fusion transition. *J Cell Biol.* 2000; 151(2):425–437. [PubMed: 11038188]
50. Hofmann MW, Peplowska K, Rohde J, Poschner BC, Ungermann C, Langosch D. Self-interaction of a SNARE Transmembrane Domain Promotes the Hemifusion-to-fusion Transition. *J Mol Biol.* 2006; 364(5):1048–1060. [PubMed: 17054985]

51. Friant S, Pecheur EI, Eugster A, Michel F, Lefkir Y, Nourrisson D, Letourneur F. Ent3p Is a PtdIns(3,5)P2 effector required for protein sorting to the multivesicular body. *Dev Cell*. 2003; 5(3):499–511. [PubMed: 12967568]
52. Collins KM, Wickner WT. Trans-SNARE complex assembly and yeast vacuole membrane fusion. *Proc Natl Acad Sci U S A*. 2007; 104(21):8755–8760. [PubMed: 17502611]
53. Stroupe C, Collins KM, Fratti RA, Wickner W. Purification of active HOPS complex reveals its affinities for phosphoinositides and the SNARE Vam7p. *Embo J*. 2006; 25(8):1579–1589. [PubMed: 16601699]
54. Wang J, Gossing M, Fang P, Zimmermann J, Li X, von Mollard GF, Niu L, Teng M. Epsin N-terminal homology domains bind on opposite sides of two SNAREs. *Proc Natl Acad Sci U S A*. 2011; 108(30):12277–12282. [PubMed: 21746902]
55. Zimmermann J, Chidambaram S, Fischer von Mollard G. Dissecting Ent3p: the ENTH domain binds different SNAREs via distinct amino acid residues while the C-terminus is sufficient for retrograde transport from endosomes. *Biochem J*. 2010; 431(1):123–134. [PubMed: 20658963]
56. Alpadi K, Kulkarni A, Comte V, Reinhardt M, Schmidt A, Namjoshi S, Mayer A, Peters C. Sequential analysis of trans-SNARE formation in intracellular membrane fusion. *PLoS Biol*. 2012; 10(1):e1001243. [PubMed: 22272185]
57. Das S, Rand RP. Diacylglycerol causes major structural transitions in phospholipid bilayer membranes. *Biochem Biophys Res Commun*. 1984; 124(2):491–496. [PubMed: 6541910]
58. Seddon JM. An inverse face-centered cubic phase formed by diacylglycerol-phosphatidylcholine mixtures. *Biochemistry*. 1990; 29(34):7997–8002. [PubMed: 2261457]
59. Simons K, Toomre D. Lipid rafts and signal transduction. *Nat Rev Mol Cell Biol*. 2000; 1(1):31–39. [PubMed: 11413487]
60. Lang T. SNARE proteins and ‘membrane rafts’. *J Physiol*. 2007; 585(Pt 3):693–698. [PubMed: 17478530]
61. Mazelova J, Ransom N, Astuto-Gribble L, Wilson MC, Deretic D. Syntaxin 3 and SNAP-25 pairing, regulated by omega-3 docosahexaenoic acid, controls the delivery of rhodopsin for the biogenesis of cilia-derived sensory organelles, the rod outer segments. *J Cell Sci*. 2009; 122(Pt 12):2003–2013. [PubMed: 19454479]
62. Darios F, Wasser C, Shakirzyanova A, Giniatullin A, Goodman K, Munoz-Bravo JL, Raingo J, Jorgacevski J, Kreft M, Zorec R, Rosa JM, Gandia L, Gutierrez LM, Binz T, Giniatullin R, Kavalali ET, Davletov B. Sphingosine facilitates SNARE complex assembly and activates synaptic vesicle exocytosis. *Neuron*. 2009; 62(5):683–694. [PubMed: 19524527]
63. Chang J, Kim SA, Lu X, Su Z, Kim SK, Shin YK. Fusion step-specific influence of cholesterol on SNARE-mediated membrane fusion. *Biophys J*. 2009; 96(5):1839–1846. [PubMed: 19254542]
64. Linetti A, Fratangeli A, Taverna E, Valnegri P, Francolini M, Cappello V, Matteoli M, Passafaro M, Rosa P. Cholesterol reduction impairs exocytosis of synaptic vesicles. *J Cell Sci*. 2010; 123(Pt 4):595–605. [PubMed: 20103534]
65. Fraldi A, Annunziata F, Lombardi A, Kaiser HJ, Medina DL, Spampanato C, Fedele AO, Polishchuk R, Sorrentino NC, Simons K, Ballabio A. Lysosomal fusion and SNARE function are impaired by cholesterol accumulation in lysosomal storage disorders. *EMBO J*. 2010; 29(21):3607–3620. [PubMed: 20871593]
66. Lam AD, Tryoen-Toth P, Tsai B, Vitale N, Stuenkel EL. SNARE-catalyzed fusion events are regulated by Syntaxin1A-lipid interactions. *Mol Biol Cell*. 2008; 19(2):485–497. [PubMed: 18003982]
67. Mima J, Wickner W. Phosphoinositides and SNARE chaperones synergistically assemble and remodel SNARE complexes for membrane fusion. *Proc Natl Acad Sci U S A*. 2009; 106(38):16191–16196. [PubMed: 19805279]
68. Liu S, Wilson KA, Rice-Stitt T, Neiman AM, McNew JA. In vitro fusion catalyzed by the sporulation-specific t-SNARE light-chain Spo20p is stimulated by phosphatidic acid. *Traffic*. 2007; 8(11):1630–1643. [PubMed: 17714435]
69. Lemmon MA. Membrane recognition by phospholipid-binding domains. *Nat Rev Mol Cell Biol*. 2008; 9(2):99–111. [PubMed: 18216767]

70. Giocondi MC, Yamamoto D, Lesniewska E, Milhiet PE, Ando T, Le Grimellec C. Surface topography of membrane domains. *Biochim Biophys Acta*. 2010; 1798(4):703–718. [PubMed: 19796628]
71. Kozlovsky Y, Chernomordik LV, Kozlov MM. Lipid intermediates in membrane fusion: formation, structure, and decay of hemifusion diaphragm. *Biophys J*. 2002; 83(5):2634–2651. [PubMed: 12414697]
72. Stein A, Weber G, Wahl MC, Jahn R. Helical extension of the neuronal SNARE complex into the membrane. *Nature*. 2009; 460(7254):525–528. [PubMed: 19571812]
73. Lewis JL, Dong M, Earles CA, Chapman ER. The transmembrane domain of syntaxin 1A is critical for cytoplasmic domain protein-protein interactions. *J Biol Chem*. 2001; 276(18):15458–15465. [PubMed: 11278966]
74. Thorngren N, Collins KM, Fratti RA, Wickner W, Merz AJ. A soluble SNARE drives rapid docking, bypassing ATP and Sec17/18p for vacuole fusion. *Embo J*. 2004; 23:2765–2776. [PubMed: 15241469]
75. Seeley ES, Kato M, Morgolis N, Wickner W, Eitzen G. Genomic analysis of homotypic vacuole fusion. *Mol Biol Cell*. 2002; 13(3):782–794. [PubMed: 11907261]
76. Parrish WR, Stefan CJ, Emr SD. Essential role for the myotubularin-related phosphatase Ymr1p and the synaptojanin-like phosphatases Sjl2p and Sjl3p in regulation of phosphatidylinositol 3-phosphate in yeast. *Mol Biol Cell*. 2004; 15(8):3567–3579. [PubMed: 15169871]
77. Ungermann C, Nichols BJ, Pelham HR, Wickner W. A vacuolar v-t-SNARE complex, the predominant form in vivo and on isolated vacuoles, is disassembled and activated for docking and fusion. *J Cell Biol*. 1998; 140(1):61–69. [PubMed: 9425154]
78. Haas A, Wickner W. Homotypic vacuole fusion requires Sec17p (yeast alpha-SNAP) and Sec18p (yeast NSF). *Embo J*. 1996; 15(13):3296–305. [PubMed: 8670830]
79. Nichols BJ, Ungermann C, Pelham HR, Wickner WT, Haas A. Homotypic vacuolar fusion mediated by t- and v-SNAREs. *Nature*. 1997; 387(6629):199–202. [PubMed: 9144293]
80. Johnson JE, Giorgione J, Newton AC. The C1 and C2 domains of protein kinase C are independent membrane targeting modules, with specificity for phosphatidylserine conferred by the C1 domain. *Biochemistry*. 2000; 39(37):11360–11369. [PubMed: 10985781]
81. Gillooly DJ, Morrow IC, Lindsay M, Gould R, Bryant NJ, Gaullier JM, Parton RG, Stenmark H. Localization of phosphatidylinositol 3-phosphate in yeast and mammalian cells. *Embo J*. 2000; 19(17):4577–4588. [PubMed: 10970851]
82. Rosenthal JA, Chen H, Slepnev VI, Pellegrini L, Salcini AE, Di Fiore PP, De Camilli P. The epsins define a family of proteins that interact with components of the clathrin coat and contain a new protein module. *J Biol Chem*. 1999; 274(48):33959–33965. [PubMed: 10567358]
83. Taylor GS, Maehama T, Dixon JE. Inaugural article: myotubularin, a protein tyrosine phosphatase mutated in myotubular myopathy, dephosphorylates the lipid second messenger, phosphatidylinositol 3-phosphate. *Proc Natl Acad Sci U S A*. 2000; 97(16):8910–8915. [PubMed: 10900271]
84. Marcus SL, Wenk MR, Steele-Mortimer O, Finlay BB. A synaptojanin-homologous region of *Salmonella typhimurium* SigD is essential for inositol phosphatase activity and Akt activation. *FEBS Lett*. 2001; 494(3):201–207. [PubMed: 11311241]
85. Wang L, Merz AJ, Collins KM, Wickner W. Hierarchy of protein assembly at the vertex ring domain for yeast vacuole docking and fusion. *J Cell Biol*. 2003; 160(3):365–374. [PubMed: 12566429]
86. Starai VJ, Jun Y, Wickner W. Excess vacuolar SNAREs drive lysis and Rab bypass fusion. *Proc Natl Acad Sci U S A*. 2007; 104(34):13551–13558. [PubMed: 17699614]
87. Haas A, Conradt B, Wickner W. G-protein ligands inhibit in vitro reactions of vacuole inheritance. *J Cell Biol*. 1994; 126(1):87–97. [PubMed: 8027189]
88. Haas A, Scheglmann D, Lazar T, Gallwitz D, Wickner W. The GTPase Ypt7p of *Saccharomyces cerevisiae* is required on both partner vacuoles for the homotypic fusion step of vacuole inheritance. *Embo J*. 1995; 14(21):5258–5270. [PubMed: 7489715]

Abbreviations used

CBP	Calmodulin binding peptide
CPZ	chlorpromazine
LPC	Lysophosphatidylcholine
PX	Phox homology domain
SNARE	soluble N-ethylmaleimide-sensitive factor attachment protein receptors
SNAP	soluble NSF attachment protein

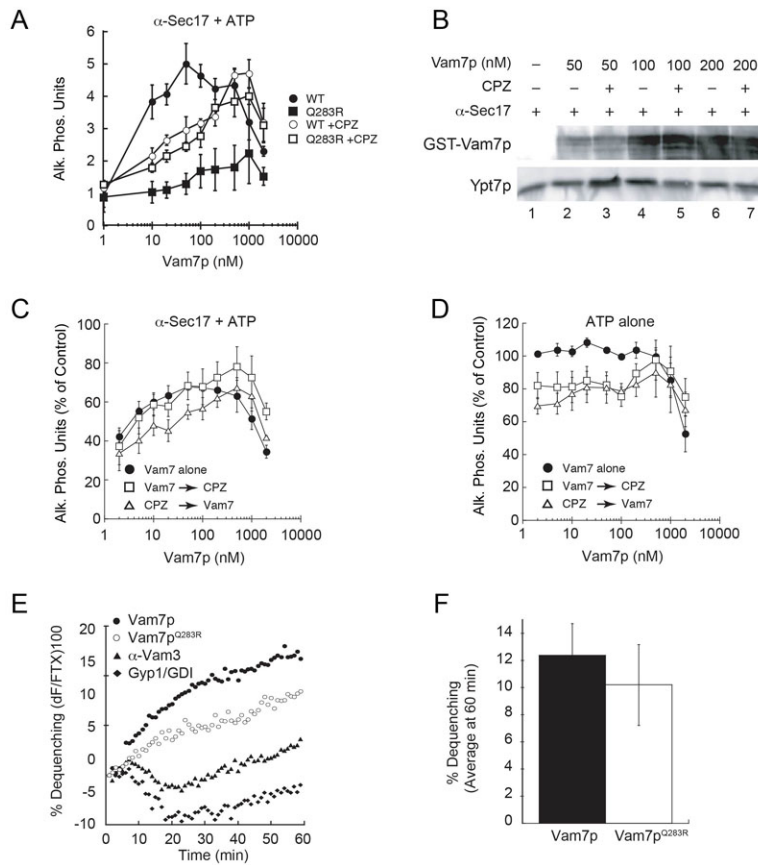


Figure 1. Non-canonical SNARE complexes stall at a hemifusion intermediate
 (A) Individual fusion reactions were blocked at the priming stage by treating vacuoles with 85 μ g/ml anti-Sec17p antibody for 15 minutes. Recombinant Vam7p (closed circles) or Vam7p^{Q283R} (closed squares) was added to bypass the priming block. In parallel, Vam7p and Vam7p^{Q283R} were added to reactions blocked with anti-Sec17p antibody and before treatment with CPZ. (B) Fusion reactions were treated with anti-Sec17p antibody in the presence or absence of CPZ. Next, recombinant Vam7p was added to reactions at the indicated concentrations. After incubation (10 minutes, 27°C), membranes were pelleted (16,000 g, 10 minutes, 4°C) and the unbound Vam7p was discarded with the supernatant. Bound Vam7p was examined by immunoblotting. Membranes were also probed for Ypt7p as a control for loading. (C) Fusion reactions were treated with anti-Sec17 antibody after which Vam7p alone (closed circles) was added to bypass the fusion block. In parallel, reactions were treated with CPZ either before (open triangles) or after addition of Vam7p (open squares). (D) Uninhibited fusion reactions were treated with Vam7p alone (closed circles). In parallel, reactions were treated with CPZ either before (open triangles) or after addition of Vam7p (open squares). (E) Lipid mixing (hemifusion) assays were performed using vacuoles blocked with anti-Sec17p at 4°C. After 15 minutes, 400 nM Vam7p (WT or Q283R) was added to the indicated reactions while on ice prior to transferring to the plate to 27°C and further incubation (60 minutes). The increase in fluorescence occurred when the outer leaflets of vacuoles were mixed during hemifusion. Shown is a representative of 3 trials. (F) Shown is the average lipid dequenching at 60 minutes. Error bars indicate SEM (n=3).

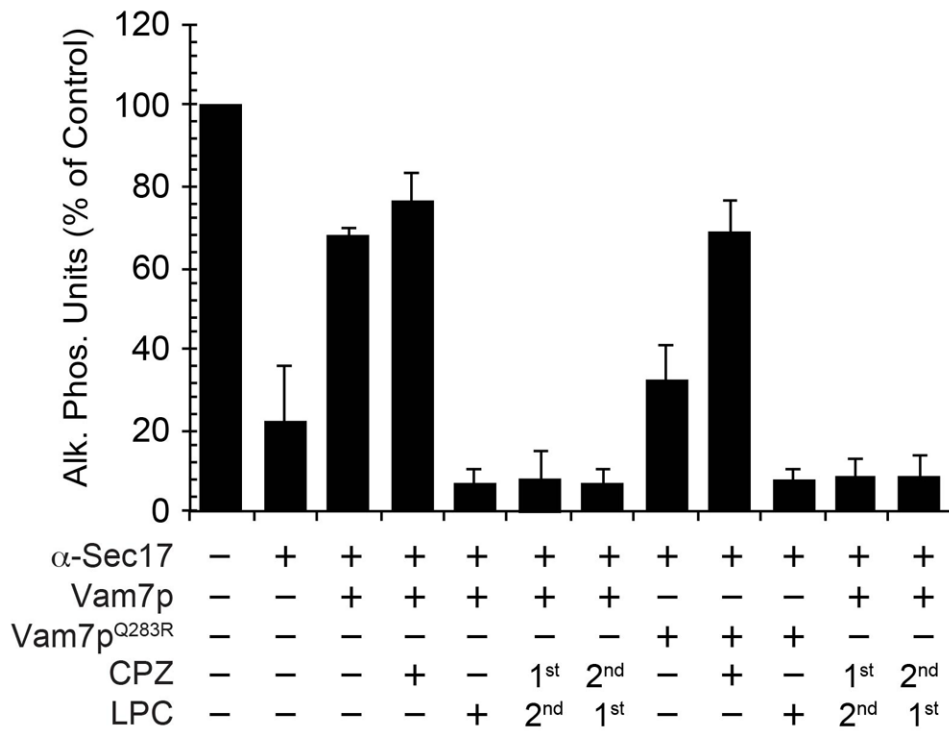


Figure 2. Lysophosphatidylcholine inhibits the Vam7p bypass of anti-Sec17p IgG blocked fusion reactions

Fusion reactions were treated with buffer or blocked with anti-Sec17p antibody. Reactions were further treated with 150 μM CPZ or 0.033% LPC for 5 minutes preceding the addition of recombinant Vam7p or Vam7p^{Q283R}. In parallel, anti-Sec17p antibody blocked vacuoles were treated with CPZ for 5 minutes followed by LPC for 5 minutes or vice versa before the addition of 400 nM Vam7p or Vam7p^{Q283R}. Error bars represent SEM (n=3)

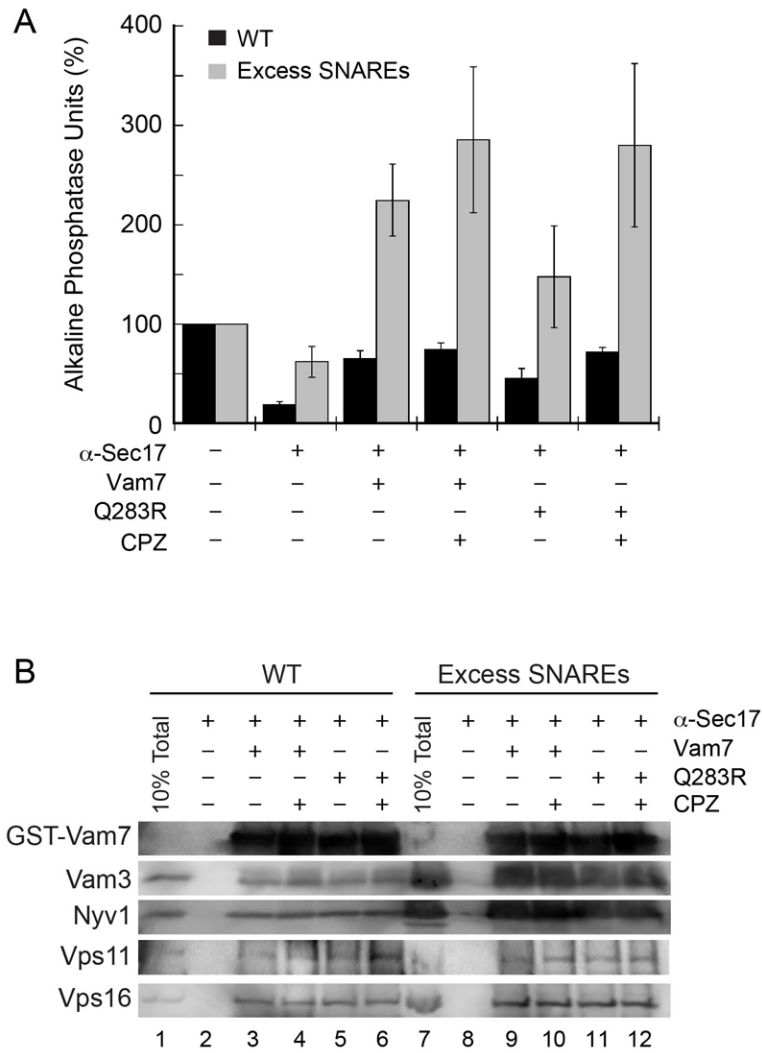


Figure 3. Non-canonical SNARE complexes support fusion when their surface density is increased

(A) Standard fusion reactions containing vacuoles from wild type strains (black bars) or SNARE overexpressing strains (gray bars) were blocked at the priming stage with 85 μg/ml anti-Sec17p antibody for 15 minutes. Recombinant GST-Vam7p (400 nM, black bars) or Vam7p^{Q283R} (gray bars) was added to bypass the priming block. Error bars represent SEM (n=3). (B) GST-Vam7p protein complexes were isolated as described in the Materials and Methods section and examined by immunoblotting for the indicated proteins.

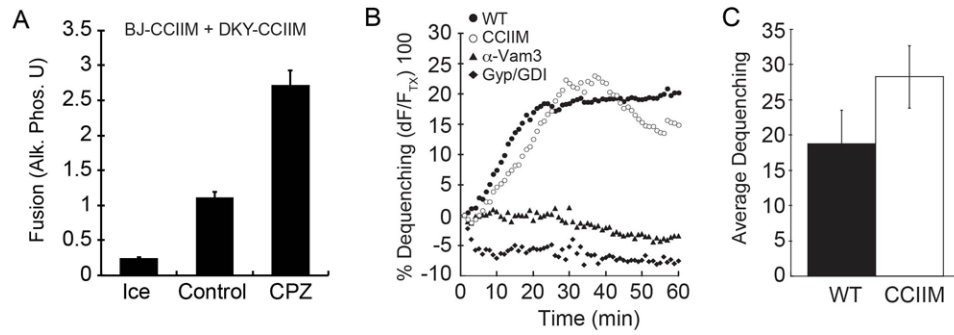


Figure 4. CPZ augments fusion of vacuoles containing lipid-anchored Vam3p

(A) Standard fusion reactions were performed using vacuoles from DKY6281 and BJ3505 strains harboring Vam3p-CCIIM. Fusion reactions were treated with buffer (Control) or CPZ and incubated for 90 minutes and fusion was measured by content mixing and Pho8p activity. (B) Lipid mixing (hemifusion) assays were performed using WT or Vam3p-CCIIM vacuoles as described in the Materials and Methods section and Figure 1. WT vacuoles were also treated with anti-Sec17 to block SNARE priming. Reactions were incubated for 60 minutes at 27°C. Shown is a representative of 3 trials. The inset represents the average lipid dequenching at 60 minutes. Error bars indicate SEM (n=3). (C) Shown is the average lipid dequenching at 60 minutes. Error bars indicate SEM (n=3).

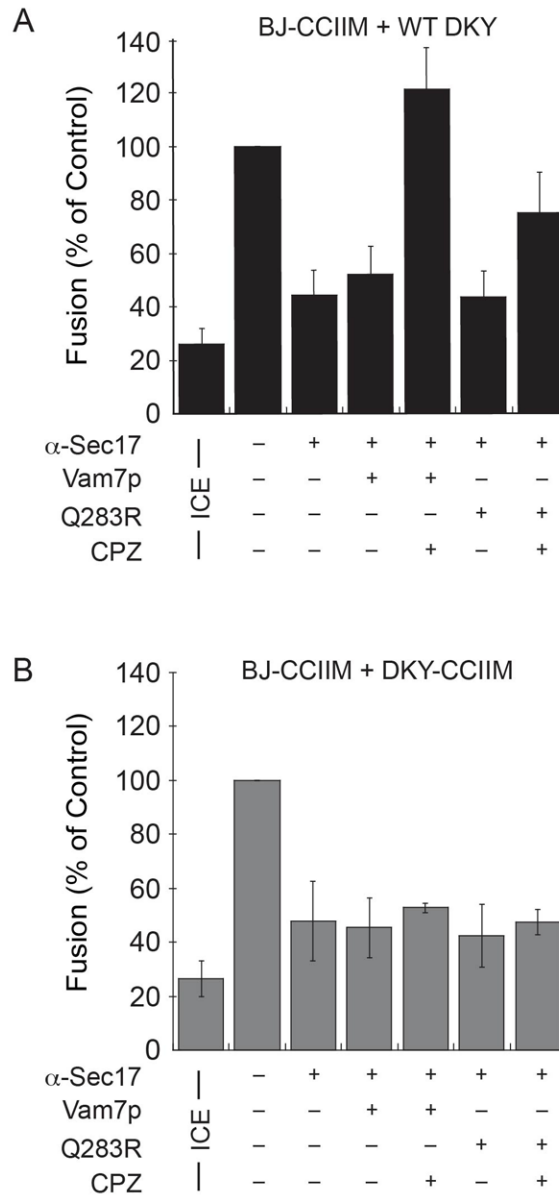


Figure 5. CPZ and Vam7p bypass anti-Sec17p IgG-blocked fusion of vacuoles containing lipid-anchored Vam3p

(A) Vacuoles from wild type DKY6281 were incubated with BJ3505 vacuoles harboring Vam3p-CCIIM. Priming was blocked with anti-Sec17p antibody for 15 minutes and reactions were treated with 150 μ M CPZ for 5 minutes before the addition of 400 nM Vam7p or Vam7p^{Q283R}. (B) Fusion reactions were performed with DKY6281 and BJ3505 vacuoles harboring Vam3p-CCIIM. Fusion reactions were treated with CPZ and Vam7p as described in (A). Error bars represent SEM (n=3).

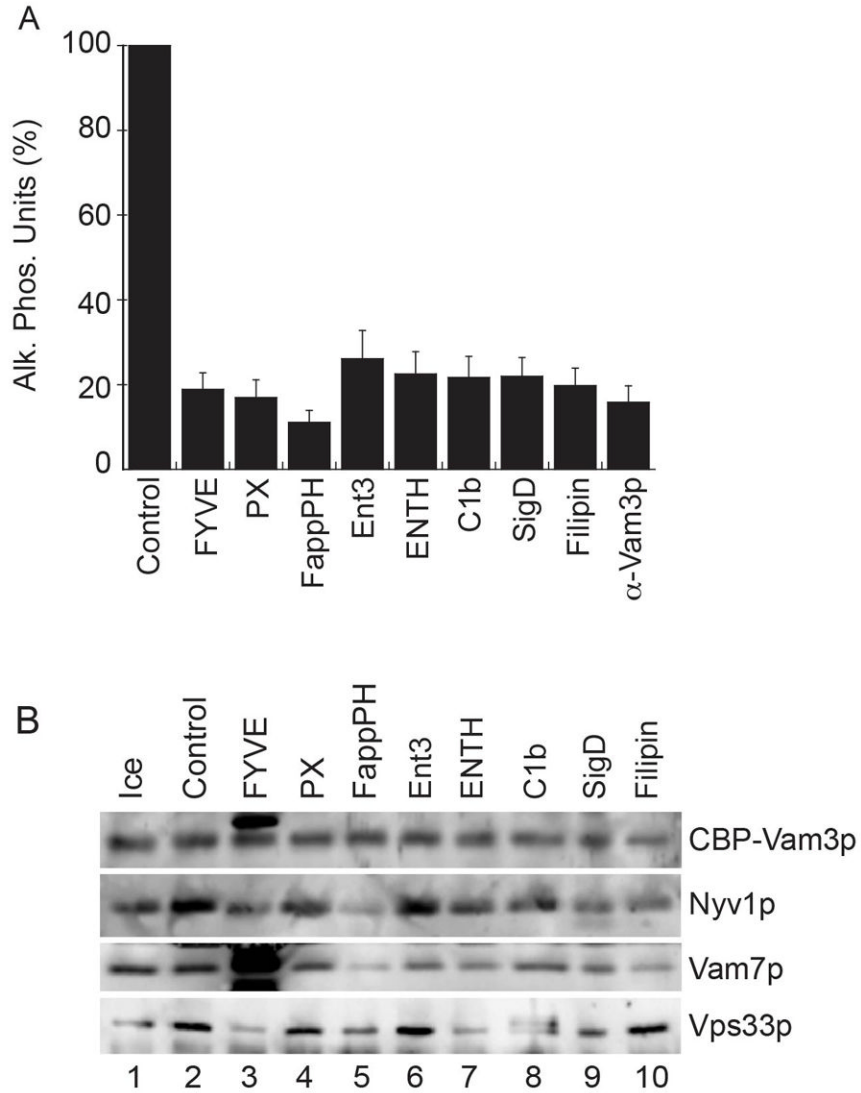


Figure 6. Regulatory lipids affect *trans*-SNARE complex formation and interactions with the HOPS complex

16X standard fusion reactions containing 48 μ g of BJ3505 CBP-Vam3p *nyv1* Δ vacuoles and 48 μ g DK6281 vacuoles were treated with inhibitory concentrations of the following lipid binding domains: 2 μ M GST-FYVE, 25 μ M GST-PX, 1 μ M MBP-FappPH, 10 μ M Ent3p-ENTH, 10 μ M Epsin1-ENTH, 10 μ M GST-C1b, 2 μ M His₆-SigD or 20 μ M filipin for 90 minutes at 27°C. (A) Samples (30 μ l) were withdrawn from each reaction to measure Pho8p activity following fusion. Error bars represent SEM (n=3). (B) The reaction remainders were centrifuged to isolate the vacuoles. Membranes were then solubilized and CBP-Vam3p complexes were affinity purified using calmodulin agarose as described in the Materials and Methods. *Trans*-SNARE complexes were detected by immunoblotting for Vam3p, Nyv1p and Vam7p. The Image shown is representative of 3 independent trials.

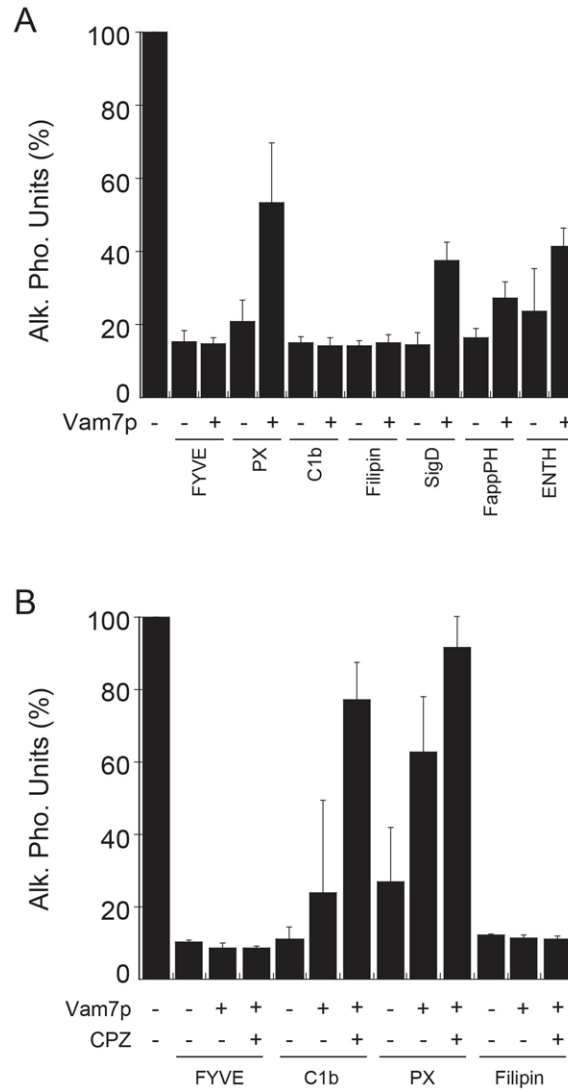


Figure 7. Vam7p and CPZ can bypass fusion blocked by specific lipid ligands
 (A) Fusion reactions were treated for 5 minutes with lipid binding domains including GST-FYVE, GST-PX, GST-C1b, Filipin, His₆-SigD, MBP-FappPH and Ent3p-ENTH as described in Fig. 5. Next, Vam7p (400 nM) was added to the reactions and incubated for a total of 90 minutes. Fusion was tested by content mixing and Pho8p activity. (B) Fusion reactions were treated for 5 minutes with lipid binding domains including. Next, 150 μM CPZ was added and the reactions were incubated for an additional 5 minutes before the addition of 400 nM Vam7p. Error bars represent SEM (n=3).